

RELATIVE OPTIMALITY CONDITIONS AND ALGORITHMS FOR TREESPACE FRÉCHET MEANS*

SEAN SKWERER[†], SCOTT PROVAN[‡], AND J.S. MARRON[§]

Abstract. Recent interest in treespaces as well-founded mathematical domains for phylogenetic inference and statistical analysis for populations of anatomical trees has motivated research into efficient and rigorous methods for optimization problems on treespaces. A central problem in this area is computing an average of phylogenetic trees, which is equivalently characterized as the minimizer of the Fréchet function. The Fréchet mean can be used for statistical inference and exploratory data analysis: for example it can be leveraged as a test statistic to compare groups via permutation tests, or to find trends in data over time via kernel smoothing. By analyzing the differential properties of the Fréchet function along geodesics in treespace we obtained a theorem describing a decomposition of the derivative along a geodesic. This decomposition theorem is used to formulate optimality conditions which are used as a logical basis for an algorithm to verify relative optimality at points where the Fréchet function gradient does not exist.

Key words. optimization, nonlinear, combinatorics, phylogenetics, cubical complexes, trees

AMS subject classifications. 90C48, 90C90

1. Introduction. The space of phylogenetic trees introduced by Billera, Holmes and Vogtman [6] is a metric space in which each point corresponds to a hypothetical evolutionary history. This space will be referred to as BHV Treespace. Inference about the evolutionary relationships of species has been a long standing issue in biology. As such phylogenetics is a mature field, with many approaches. For book length treatments of phylogenetic inference and related mathematics see [7, 10]. A space of phylogenetic trees is a pivotal mathematical concept for sound inference of evolutionary relationships [12, 13]. Although the specific metric for a space phylogenetic trees, or scope of a space of models for evolutionary relationships to include various types of trees or other structures such as networks are issues which may not yet be completely resolved, any such space will have a non-Euclidean geometry. The solution of the Fréchet mean problem on BHV Treespace is a relevant research problem for phylogenetics and for applications involving modeling biological forms as trees. Treespace has also been used in statistical analyses where populations of lungs [9] and arteries [21] are modeled as trees. The central research problem of this paper is efficient computation of the Fréchet mean of a discrete sample of points in treespace. More specifically this paper focuses on deriving optimality conditions through the analysis of derivatives along geodesic paths issuing from singular points in treespace and an iterative interior point method for local optimization.

The main challenge here is that the Fréchet function gradient is not well-defined everywhere in treespace. The stratified structure of treespace is formed by gluing together Euclidean orthants (this is described in detail in Sec. 2.2). Gradients are not well defined at such glued points due to this non-differentiable geometry. Even if the domain of the Fréchet optimization is restricted to a single orthant of treespace while the trees T_1, \dots, T_n are supported on the entire space, the value of the Fréchet function is piecewise continuous, but not differentiable. To be precise, on the boundary of the orthant, in directions from boundary to interior, directional derivatives of the Fréchet function exist but the gradient is not well defined; and the interior of an orthant of treespace can be subdivided into regions where the Fréchet function is C^∞ differentiable on their interiors but it is only C^1 differentiable on their boundaries.

Derivative free search procedures can be used to avoid these non-differentiability issues

*Submitted to the editors November 2015.

[†] (seanskwerer@gmail.com).

[‡]Department of Statistics and Operations Research University of North Carolina Chapel Hill (provan@unc.edu).

[§]Department of Statistics and Operations Research University of North Carolina Chapel Hill (marron@unc.edu).

(discussed further in Sec. 3). These derivative free procedures are designed to converge in distance to the optimal point. When the Fréchet mean is not a completely resolved tree, these procedures, which in practice can continue only for finite number of iterations, will return trees having edges that are not present in the Fréchet mean.

When the Fréchet mean is a fully resolved tree, the gradient of the Fréchet function at that point in treespace exists, and its optimality can be confirmed by checking the gradient is zero. However, to date, there are no known quickly verifiable certificates for a treespace Fréchet mean in general. Our main results in this paper are (1) a decomposition theorem for derivatives along geodesics and (2) an algorithm to find the minimizer of the Fréchet function when the domain is restricted to a single orthant of treespace. This algorithm will determine the optimal point in a single orthant of treespace even when the optimal point represents a tree which is not fully resolved.

Essentially, our new algorithm minimizes the directional derivative of the Fréchet function over the set of all directions issuing from a point to within the closure of an orthant, and verifies that there is no direction where the derivative is negative. The crux of this approach is that when the Fréchet function gradient does not exist then generally the gradient of the directional derivative function does not exist. This issue is solved with a nested optimality condition based on recursive decomposition of the directional derivatives.

The remaining contents of this paper are organized as follows. Background about treespace and geodesics is presented in Sec. 2. In Sec. 3 we give a high-level discussion of technical issues for the Fréchet optimization problem. The main theorems are discussed in Sec. 4 (proofs are in Sec. 6). In Sec. 5 a method finding the minimizer of the Fréchet function in a fixed orthant of treespace is presented. The focus of Sec. 6 is our analysis of the differential properties of the Fréchet function. Concluding remarks and further research directions are in Sec. 7.

2. Background. Definitions and descriptions of phylogenetic trees and Billera, Holmes, and Vogtman (BHV) Treespace are given in Sec. 2.1 and Sec. 2.2. Treespace geodesics are defined in Sec. 2.3. In Sec. 2.4 we state the Fréchet mean optimization problem. In Sec. 2.5 we describe how the combinatorics of treespace geodesics lead to subdivision of treespace into regions where the Fréchet function has a fixed algebraic form.

2.1. Phylogenetic trees. Evolutionary histories or hierarchical relationships are often represented graphically as phylogenetic trees. In biology, the evolutionary history of species or operational taxonomic units (OTU's) is represented by a tree. The root of the tree corresponds to a common ancestor. Branches indicate speciation of a nearest common ancestor into two or more distinct taxa. The leaves of the tree correspond to the present species whose history is depicted by the tree. An overview of the data used in phylogenetic inference is presented in Sec. 2.1.1 and mathematical definitions for phylogenetic trees are given in Sec. 2.1.2.

2.1.1. Genetic Data for Phylogenetics. Phylogenetic trees and inferences about the evolutionary relationships of species are typically made from molecular sequence data of DNA, RNA, amino acids, or proteins, aligned for interspecies comparison. Table 1 contains a small artificial example of DNA base pair data.

In this example, the pattern in each column yields a partition of the species into two groups. Column a partitions the snakes into {King Cobra, Copper Head, Black Mamba, Corn Snake} and {Boa Constrictor, Coral Snake, Cotton Mouth}. Snakes with A (adenine) in column b are a subset of the group of snakes with A in column a, and likewise snakes with T (thymine) in column a are a subset of the group of snakes with C (cytosine) in column b. Together column a and column b partition into three groups: {King Cobra, Copper Head, Black Mamba}, {Corn Snake}, and {Boa Constrictor, Coral Snake, Cotton Mouth}. Column a and column b are an example of compatible splits (see. Sec. 2.1.2 for definition for compatible splits). On the other hand, column b and column d are an example of incompatible splits. The pattern in column b separates Black Mamba from Corn Snake, while the pattern in column d puts these snakes in the same group.

Table 1: Artificial example of nine aligned DNA base pairs from seven species of snake.

Species	a	b	c	d	e	f	g	h	i
1. King Cobra	A	A	T	A	C	T	A	A	C
2. Copper Head	A	A	T	A	G	T	T	A	G
3. Black Mamba	A	A	T	G	G	C	T	A	G
4. Corn Snake	A	C	T	G	G	C	A	A	G
5. Boa Constrictor	T	C	T	A	C	T	A	A	G
6. Coral Snake	T	C	A	G	C	T	A	A	G
7. Cotton Mouth	T	C	A	G	C	T	A	T	C

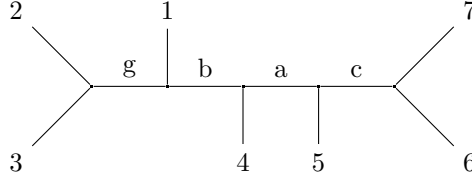


Fig. 1: A phylogenetic tree for seven species of snake from data in Table 1. This tree represents the partitions of the species into groups from columns a, b, c, and g.

A set of compatible splits can be combined into a tree. The information in columns a, b, c, g and h suggests one possible configuration of evolutionary relationships for these snake species, which is depicted as a tree in Figure 1.

The split from column d is incompatible with columns a, b, c, and g, and such conflicting information cannot be put into a single tree. Genetic data may support multiple evolutionary histories because genes, the elementary units of inheritance [11], may evolve independently from each other as they are driven by independent environmental factors. The problem of forming a species tree from gene trees is known as gene tree species tree reconciliation [14, 16].

2.1.2. Mathematical Definitions for Phylogenetic Trees. A *labeled tree* is a tree T with $r + 1$ leaves distinctly labeled using the index set $I = \{0, 1, \dots, r\}$. An edge e is characterized by a *split*, which is a partition of I into two disjoint sets of labels, X_e and \bar{X}_e . Edge e is present in tree T if and only if deleting e from T yields one subtree with leaves distinctly labeled by X_e and another subtree with leaves distinctly labeled by \bar{X}_e .

A *phylogenetic tree* is a labeled tree with weighted edges: the set of edges for a tree T is written E_T , and edge weights are a function from the edges of T to the positive real numbers, $| : E_T \rightarrow \mathbb{R}_{>0}$. The lengths of edges in a tree will typically represent some measure of genetic difference, or in some models the passage of time. When edge lengths represent the passage of time, the leafs of the tree are associated with contemporary species, while the root is associated with an ancestral species. In that case the edge lengths must be normalized so that the passage of time represented by the path from the ancestor to each contemporary species is the same. The *topology of a phylogenetic tree* is the underlying graph and leaf labels separated from the edge lengths. The topology of a phylogenetic tree is uniquely represented by the set of splits associated with its edges. Formally, two splits $X_e \cup \bar{X}_e$ and $X_f \cup \bar{X}_f$ are *compatible* if and only if $X_e \subset X_f$ and $\bar{X}_e \subset \bar{X}_f$, or $X_f \subset X_e$ and $\bar{X}_f \subset \bar{X}_e$. Compatibility can be interpreted in terms of subtrees: the subtree with leaves in bijection with \bar{X}_e contains the subtree with leaves in bijection with \bar{X}_f , or vice versa. The compatibility of splits on snake species from the aligned DNA base pairs in 1 depicted as a graph in Figure 2, with one node for each split and an edge connecting each compatible pair. If every pair of splits in a set of splits is compatible then that set is said to be a compatible set. Each distinct set of compatible splits is equivalent to a unique phylogenetic

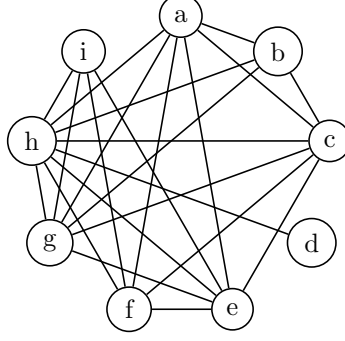


Fig. 2: Compatibility graph for splits on snake species from aligned DNA base pairs in Table 1.

$\{0, 1\} \{2, 3, 4\}$	$\{0, 1, 2\} \{3, 4\}$	$\{0, 2\} \{1, 3, 4\}$	$\{0, 2, 4\} \{1, 3\}$	$\{0, 1, 3\} \{2, 4\}$
$\{0, 1, 4\} \{2, 3\}$	$\{0, 2, 3\} \{1, 4\}$	$\{0, 3\} \{1, 2, 4\}$	$\{0, 3, 4\} \{1, 2\}$	$\{0, 4\} \{1, 2, 3\}$

Table 2: Ten partitions of $\{0, 1, 2, 3, 4\}$ which are splits for internal edges in the BHV Treespace \mathcal{T}_4 . Comptable splits are combined to make tree topologies as depicted if Fig. 3.

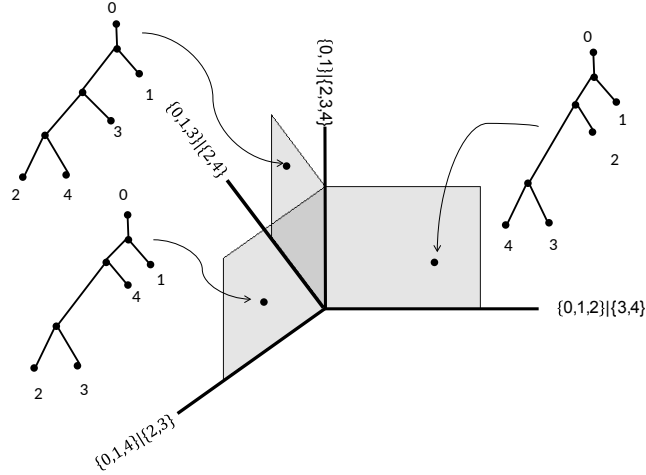
tree topology. A maximal tree topology is one in which no additional interior edges can be introduced i.e. $|E_T| = 2r - 1$, or equivalently every interior vertex has degree 3.

2.2. Construction of BHV Treespaces. A BHV Treespace, \mathcal{T}_r is a geometric space in which each point represents a phylogenetic tree having leaves in bijection with a fixed label set $\{0, 1, 2, \dots, r\}$.

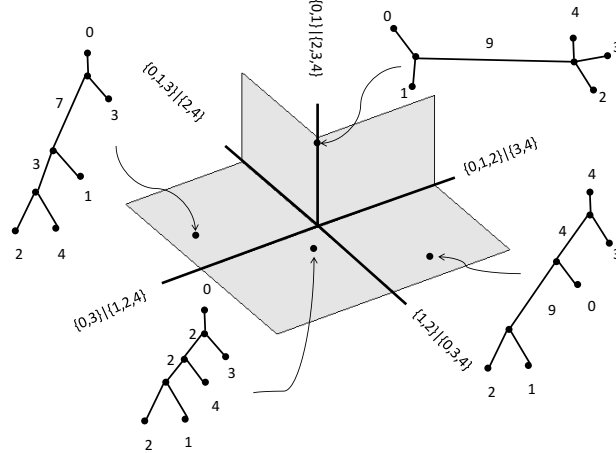
A *non-negative orthant* is a copy of the subset of n -dimensional Euclidean space defined by restricting each coordinate to non-negative values, $\mathbb{R}_{\geq 0}^n$. Here, only non-negative orthants are used, so we use orthant to mean non-negative orthant. An *open orthant* is the set of positive points in an orthant. Phylogenetic treespace is a union of many orthants, each corresponding to a distinct tree topology, wherein the coordinates of a point are interpreted as the lengths of edges. For a given set of compatible edges E , the associated orthant is denoted $\mathcal{O}(E)$, and for a given tree T , the minimal orthant in treespace containing that point is denoted $\mathcal{O}(T)$. Trees in \mathcal{T}_r have at most $r - 2$ interior edges. Each orthant of dimension $r - 2$ corresponds to a combination of $r - 2$ compatible edges. Orthants are glued together along common axes. The shared faces of facets with k positive coordinates are called the k -dimensional faces of treespace.

Take \mathcal{T}_4 as an example. There are ten possible splits (not including five leaf edges), see Table 2 for a list. These splits can be combined into fifteen distinct tree topologies, comprised of pairs of compatible splits. Each compatible pair is associated with a copy of $\mathbb{R}_{\geq 0}^2$, one axis of the orthant for each edge in the pair. These fifteen orthants are glued together along common axes. Views of two parts of \mathcal{T}_4 are displayed in Figure ?? . See Figure 4 for a visualization of the split-split compatibility graph of \mathcal{T}_4 ¹.

¹An interesting fact is that the compatibility graph of \mathcal{T}_4 is a Peterson graph.



(a) A half-open book with three pages. In this diagram the *pages* of the book are three copies of $\mathbb{R}_{\geq 0}^2$ and the *spine* is a copy of $\mathbb{R}_{\geq 0}$. The spine is labeled with the split $\{0, 1\}|\{2, 3, 4\}$. Each page has the spine as one axis and the other axis is labeled with a split compatible with $\{0, 1\}|\{2, 3, 4\}$. In \mathcal{T}_4 every one of the ten splits of $\{0, 1, 2, 3, 4\}$ is the label for the spine of a half-open book.



(b) A five-cycle. A *five-cycle* is five copies of $\mathbb{R}_{\geq 0}^2$ glued together along commonly labeled axes.

Fig. 3

Each clique in the split-split compatibility graph represents a compatible combination of splits, or equivalently the topology of a phylogenetic tree. A graph is *complete* if there is an edge between every pair of vertices. In a graph, a *clique* is a complete subgraph. Each full phylogenetic tree is a maximal clique in the split-split compatibility graph because a clique represents a set of mutually compatible splits. The split-split compatibility graph of \mathcal{T}_4 has fifteen maximal cliques, each of which is represented an edge in the graph. The split-split compatibility graph of \mathcal{T}_4 determines how the orthants of \mathcal{T}_4 are connected.

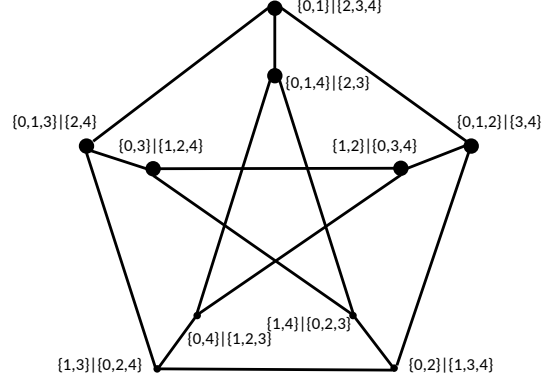


Fig. 4: Split-split compatibility graph of \mathcal{T}_4 . Each split has a node. Two splits are compatible if they are connected by an arc. This shows the overall connectivity of \mathcal{T}_4 , all possible splits for $\{0, 1, 2, 3, 4\}$, and all possible topologies for 4-trees. Each vertex and the three edges emanating from it in the graph corresponds to a copy of an open book like in Figure 3a. Each five-cycle in the graph is a copy of a five-cycle depicted in Figure 3b

The compatibility of splits from genetic sequence data in Table 1 is given in the link graph in Figure 2.

2.3. BHV Treespace geodesics. We now give an explicit description of geodesics in treespace. Let $X \in \mathcal{T}_r$ be a variable point and let $T \in \mathcal{T}_r$ be a fixed point. Let $\Gamma_{XT} = \{\gamma(\lambda) | 0 \leq \lambda \leq 1\}$ be the geodesic path from X to T . Let C be the set of edges which are compatible in both trees, that is the union of the largest subset of E_X which is compatible with every edge in T and the largest subset of E_T which is compatible with every edge in X .

The following notation for the Euclidean norm of the lengths of a set of edges A in a tree T will be used frequently,

$$(1) \quad \|A\|_T = \sqrt{\sum_{e \in A} |e|_T^2}$$

or without the subscript when it is clear to which tree the lengths are from.

A support sequence is a pair of disjoint partitions, $A_1 \cup \dots \cup A_k = E_X \setminus C$ and $B_1 \cup \dots \cup B_k = E_T \setminus C$.

THEOREM 2.1. [19] *A support sequence $(\mathcal{A}, \mathcal{B}) = (A_1, B_1), \dots, (A_k, B_k)$ corresponds to a geodesic if and only if it satisfies the following three properties:*

(P1) *For each $i > j$, A_i and B_j are compatible*

(P2) $\frac{\|A_1\|}{\|B_1\|} \leq \frac{\|A_2\|}{\|B_2\|} \leq \dots \leq \frac{\|A_k\|}{\|B_k\|}$

(P3) *For each support pair (A_i, B_i) , there is no nontrivial partition $C_1 \cup C_2$ of A_i , and partition $D_1 \cup D_2$ of B_i , such that C_2 is compatible with D_1 and $\frac{\|C_1\|}{\|D_1\|} < \frac{\|C_2\|}{\|D_2\|}$*

The geodesic between X and T can be represented in \mathcal{T}_r with legs

$$\Gamma_l = \begin{cases} \left[\gamma(\lambda) : \frac{\lambda}{1-\lambda} \leq \frac{\|A_1\|}{\|B_1\|} \right], & l = 0 \\ \left[\gamma(\lambda) : \frac{\|A_i\|}{\|B_i\|} \leq \frac{\lambda}{1-\lambda} \leq \frac{\|A_{i+1}\|}{\|B_{i+1}\|} \right], & l = 1, \dots, k-1, \\ \left[\gamma(\lambda) : \frac{\lambda}{1-\lambda} \geq \frac{\|A_k\|}{\|B_k\|} \right], & l = k \end{cases}$$

The points on each leg Γ_l are associated with tree T_l having edge set

$$E_l = B_1 \cup \dots \cup B_l \cup A_{l+1} \cup \dots \cup A_k \cup C$$

Lengths of edges in $\gamma(\lambda)$ are

$$|e|_{\gamma(\lambda)} = \begin{cases} \frac{(1-\lambda)\|A_j\| - \lambda\|B_j\|}{\|A_j\|} |e|_X & e \in A_j \\ \frac{\lambda\|B_j\| - (1-\lambda)\|A_j\|}{\|B_j\|} |e|_T & e \in B_j \\ (1-\lambda)|e|_X + \lambda|e|_T & e \in C \end{cases}.$$

The length of Γ is

$$(2) \quad d(X, T) = \sqrt{\sum_{l=1}^k (\|A_l\| + \|B_l\|)^2 + \sum_{e \in C} (|e|_X - |e|_T)^2}$$

and we call this the geodesic distance from X to T .

2.4. Fréchet means in BHV Treespace. For a given data set of n phylogenetic trees in \mathcal{T}_r , T^1, T^2, \dots, T^n , the *Fréchet function* is the sum of squares of geodesic distances from the data trees to a variable tree X . A geodesic $\gamma : [0, 1] \rightarrow \mathcal{T}_r$ is the shortest path between its endpoints. The geodesic from X to T^i is characterized by a geodesic support, $(\mathcal{A}^i, \mathcal{B}^i) = ((A_1^i, B_1^i), \dots, (A_{k^i}^i, B_{k^i}^i))$ [19]. Given the geodesic supports $(\mathcal{A}^1, \mathcal{B}^1), \dots, (\mathcal{A}^n, \mathcal{B}^n)$ the Fréchet function is

$$(3) \quad F(X) = \sum_{i=1}^n d(X, T^i)^2 = \sum_{i=1}^n \left(\sum_{l=1}^{k^i} (\|A_l^i\| + \|B_l^i\|)^2 + \sum_{e \in C^i} (|e|_X - |e|_{T^i})^2 \right)$$

The objective is to solve the Fréchet optimization problem

$$(4) \quad \min_{X \in \mathcal{T}_r} F(X)$$

Elementary Fréchet function properties:

- The Fréchet function is continuous because the geodesic distances $d(X, T^i)$ are continuous [19, 17].
- The Fréchet function $F(X)$ is strictly convex [22], that is $F \circ \gamma : [0, 1] \rightarrow \mathbb{R}$ is strictly convex for every geodesic $\gamma(\lambda)$ in \mathcal{T}_r .

As a consequence of these properties we have the following result.

LEMMA 2.2. *The Fréchet mean exists and is unique.*

Proof. A strictly convex function either has a unique minimizer or can be made arbitrarily low. Assuming that the data points are finite, then a minimizer of the Fréchet function must also be finite. Therefore the Fréchet function has a unique minimizer. \square

DEFINITION 2.3. *The Fréchet mean, \bar{T} , is the unique minimizer of the Fréchet function.*

2.5. Vistal subdivision of treespace. The value of the Fréchet function at X depends on the geodesics from X to each of the data trees. Treespace can be subdivided into regions where the combinatorial form of geodesics from X to the data trees are all fixed. Given a source tree T , a vistal facet is a region of treespace, \mathcal{V} , where a fixed support is valid for the geodesic from any tree X in \mathcal{V} to T .

DEFINITION 2.4. [17, Def. 3.3] *Let T be a tree in \mathcal{T}_r . Let \mathcal{O} be a maximal orthant containing T . The previstal facet, $\mathcal{V}(T, \mathcal{O}; \mathcal{A}, \mathcal{B})$, is the set of variable trees, $X \in \mathcal{O}$, for which the geodesic joining X to T has support $(\mathcal{A}, \mathcal{B})$ satisfying (P2) and (P3) with strict inequalities.*

A pre-multi-vistal facet is an intersection of previstal facets of T^1, \dots, T^n . Pre-multi-vistal facets are regions where the Fréchet function can be represented with a fixed algebraic form. Analysis of the differential properties of the Fréchet function at points on shared faces of pre-multi-vistal facets is important for Thm. 4.3. For deeper analysis of the geometry and combinatorics of vistal facets see [17].

3. Problem Discussion. The Fréchet optimization problem, in BHV Treespace, requires both selecting the minimizing tree topology and specifying its edge lengths. Tree topologies are discrete and so the problem of selecting the minimizing tree topology is a combinatorial optimization problem; however it is possible to make search strategies which take advantage of the continuity of BHV Treespace to find the correct tree topology. It is natural to consider this problem in two modes of search: global i.e. strategies which change the topology and edge lengths; and local i.e. strategies which only adjust edge lengths. One motivation to consider global search and local search separately is that the local optimization problem is convex optimization constrained to a Euclidean orthant.

The global search problem is challenging because the geometry of treespace creates difficulty in two essential parts of optimization (1) making progress towards optimality and (2) verifying optimality. In treespace a metrically small neighborhood can actually be quite large in a certain sense. In constructing the space, the topological identification of the shared faces of orthants may create points in the closure of many orthants. In terms of trees, the neighborhood around a tree X , $N(X)$, is comprised not only of trees with the same topology as X but also trees which have X as a contraction. However, the list of tree topologies which have a particular tree X as a contraction can be quite large. For example, if X is a star tree then X is a contraction of any tree i.e. X is a contraction of $(2r - 3)!!$ maximal phylogenetic tree topologies.

Local optimality conditions for non-differentiable functions are based on the rate of change of the objective function along directions issuing from a point. Since the neighborhood of a point X contains all trees which have X as a contraction verifying that X is optimal requires demonstrating that any tree which contains X as a contraction has a larger Fréchet function value. For example, when X is a star tree, $N(X)$ contains every tree with the same leaf edges as X , and having infinitesimal interior edge lengths. In this sense finding a descent direction can be essentially as hard as finding the topology of the Fréchet mean itself. Although exhaustive search among all possible tree topologies will eventually yield the Fréchet mean, there are more practical approaches.

Proximal point algorithms, a broad class of algorithms, are globally convergent not only for the Fréchet optimization problem, but are globally convergent for any well defined lower-semicontinuous convex optimization problem on a globally non-positively curved metric space [1]. A globally non-positively curved metric space has a unique shortest path, called a geodesic, between any pair of points. This class of algorithms has nice theoretical properties and certain implementations of proximal point algorithms are practical for the Fréchet optimization problem on globally non-positively curved orthant spaces. Orthant spaces are generalizations of treespace where the link at the origin can be an arbitrary graph, rather than a graph encoding valid phylogenetic trees [17, Sec. 6.3].

Proximal point algorithms are applicable to optimization problems on metric spaces. The general problem is minimizing a function f on a metric space M with distance function $d : M \times M \rightarrow \mathbb{R}$. A proximal point algorithm solves a sequence of penalized optimization problems of the form

$$(5) \quad P_k(f) : \min_{x^k} f(x^k) + \alpha_k d^2(x^{k-1}, x^k)$$

where α_k influences the proximity of a solution to the point x^{k-1} . Some good references for proximal point algorithms are [3, 5, 15, 20].

Global methods for optimizing the Fréchet function i.e. methods which can move from one orthant of treespace to another have been shown to converge [4, 22, 17].

Implementing a generic proximal point algorithm to minimize the Fréchet function on treespace does not seem advantageous. In particular, given a non-optimal point X^0 finding a point X such that $F(X) < F(X^0)$ is not made any easier by penalizing the objective function $F(X) + \alpha d^2(X^0, X)$. Penalizing the objective function with $\alpha d(X^0)$ does not provide any additional structure for checking the neighborhood of X^0 , $N(X^0)$, for a descent direction.

Split proximal point algorithms avoid directly tackling the complicated problem of minimizing $F(X)$ by solving many much easier subproblems. For objective functions which can

be expressed as a sum of functions, $f = f^1 + \dots + f^m$, a split proximal point algorithm alternates among penalized optimization problems for each function. Let $\{1, 2, \dots, m\}$ index the functions f^1, \dots, f^m . A generic split proximal point algorithm is: choose some sequence i_1, i_2, \dots where each term in the sequence is an element of $\{1, 2, \dots, m\}$ and sequentially solve the split proximal point optimization problem:

$$(6) \quad P_k(f^{i_k}) : \min_{x^k} f^{i_k}(x^k) + \alpha_k d^2(x^{k-1}, x^k)$$

Different versions of split proximal point algorithms are based on the choice of the sequence i_1, i_2, \dots and the choice of the sequence $\{\alpha_k\}$. Naturally, a split proximal point procedure can be applied to the Fréchet optimization problem by separating the Fréchet function into a sum of squared distance functions, $F(X) = d^2(X, T^1) + \dots + d^2(X, T^n)$. For the Fréchet function the split proximal point optimization problem is

$$(7) \quad P_k(d^2(X^k, T^{i_k})) : \min_{x^k} d^2(X^k, T^{i_k}) + \alpha_k d^2(X^{k-1}, X^k)$$

For the Fréchet mean optimization problem on a globally non-positively curved metric space, the solution to a split proximal point optimization problem can be obtained easily in terms of geodesics. The solution to $P_k(d^2(X^k, T^{i_k}))$ must be on the geodesic between X^{k-1} and T^{i_k} . The term $d^2(X^k, T^{i_k})$ is the squared distance from the variable point to T^{i_k} and the term $d^2(x^{k-1}, x^k)$ is the squared distance from the search point to X^{k-1} . Given any point, there is at least one point on the geodesic between X^{k-1} and T^{i_k} for which the value of both terms is at least as small. Since X^k must be on this geodesic, the distance from X^k to X^{k-1} and the distance from X^k to T^{i_k} can be parameterized in terms of the proportion, $t : 0 \leq t \leq 1$, along the geodesic from X^{k-1} to T^{i_k} : $d(X^k, T^{i_k}) = (1 - t)d(X^{k-1}, T^{i_k})$ and $d(X^k, X^{k-1}) = td(X^{k-1}, T^{i_k})$. Parameterizing $d^2(X^k, T^{i_k}) + \alpha_k d^2(X^{k-1}, X^k)$ in terms of t makes $P_k(d^2(X^k, T^{i_k}))$ into a problem of minimizing a quadratic function in t . The optimal step length is $t = \frac{\alpha}{1+\alpha}$. An analogous formulation of SPPA can be made for the Fréchet Median problem. Even more importantly, several versions of split proximal point algorithms have been shown to converge globally to the Fréchet mean [2].

One strategy for minimizing the Fréchet function is use a split proximal point algorithm for global search and switch to a local search procedure. The motivation for switching to a local search procedure is that if local search is initialized close to the optimal solution then faster convergence can be achieved. The local optimization problem is minimizing the Fréchet function in a fixed orthant \mathcal{O} . One feature of the local optimization problem is that the Fréchet function is C^∞ in the interior of each pre-multi-vistal cell, but not at points on shared faces of pre-multi-vistal facets. The Fréchet function is C^1 only when restricted to the interior of a maximal orthant. An analysis of differential properties of the Fréchet function is presented in Sec. 6.

4. Decomposition and Relative Optimality Theorems. The main analytical results related to minimizing $F(X)$ for a given a set of trees T^1, \dots, T^n in \mathcal{T}_r are presented in this section, and proofs are presented in Sec. 6. Each tree T^i induces pre-vistal facets on treespace and taken together the collection subdivides treespace into pre-multi-vistal facets where the Fréchet function can be represented in a fixed form. On the shared faces of pre-vistal facets the Fréchet function can be represented in multiple valid forms. At such points the value of the Fréchet function and gradient are the same, but higher order derivatives can differ depending on which representation of the Fréchet function is used. Thus careful consideration of the differential properties of the Fréchet function at such points is necessary for the Directional Derivative Decomposition Theorem (Thm. 4.3)

4.1. Decomposition Theorem. Let X and Y be points in \mathcal{T}_r such that X and Y share a pre-multi-vistal facet defined by geodesics from X to T^1, \dots, T^n , $\mathcal{V}(T^1, \mathcal{O}; \mathcal{A}^1, \mathcal{B}^1) \cap \dots \cap \mathcal{V}(T^n, \mathcal{O}; \mathcal{A}^n, \mathcal{B}^n)$. If this is the case, then either (i) X and Y have the same topology, (ii) X is a contraction of Y or (iii) Y is a contraction of X . Assume that if the topologies of

trees X and Y differ then X is a contraction of Y , that is $\mathcal{O}(X) \subseteq \mathcal{O}(Y)$. Let $\Gamma(X, Y; \alpha)$, where $0 \leq \alpha \leq 1$, be the point α proportion along the geodesic from X to Y .

DEFINITION 4.1. *The directional derivative from X to Y is*

$$(8) \quad F'(X, Y) = \lim_{\alpha \rightarrow 0} \frac{F(\Gamma(X, Y; \alpha)) - F(X)}{\alpha}$$

DEFINITION 4.2. *Let $\mathcal{O}^\perp(X)$ be the orthogonal space to $\mathcal{O}(X)$ at X , that is the union of all orthogonal spaces in all orthants containing $\mathcal{O}(X)$.*

An example of an orthogonal space can be seen in the half-open book with three pages illustrated in Fig. 3a. Consider a point X on the spine of the half-open book, labeled $\{0, 1\} \cup \{2, 3, 4\}$. The orthogonal space at X in one page of the book is a copy of the positive real line, and the complete orthogonal space at X is three copies of the positive real line, one copy identified with each page of the open book.

Thm. 4.3 states that the value of the directional derivative can be decomposed into a contribution from the change in $F(X)$ resulting in adjusting positive length edges in X , and a contribution from the change in $F(X)$ resulting in increasing the lengths of edges from zero.

THEOREM 4.3. (*Decomposition Theorem for Directional Derivatives*) *Let $X, Y \in \mathcal{T}_r$, with $\mathcal{O}(X) \subseteq \mathcal{O}(Y)$ and with X and Y in a common multi-vistal cell, V_{XY} , let Y_X be the projection of Y onto $\mathcal{O}(X)$, and let Y_\perp be the projection of Y onto $\mathcal{O}^\perp(X)$ at X . Then,*

$$(9) \quad F'(X, Y) = F'(X, Y_X) + F'(X, Y_\perp)$$

See Sec. 6 for proof and see supplemental material for an example.

4.2. Orthant optimization. Consider a variable tree $X \in \mathcal{T}_r$ and a fixed set of compatible edges E . The goal is to minimize the Fréchet function but under the restriction that the topology of X may only have edges from E . Under this restriction, the geometric location of X is restricted to the orthant defined by the set of edges E , $\mathcal{O}(E)$. As the edge lengths of X vary the geodesic from X to T^i will also vary, and the support sequence $(A^i, B^i) = (A_1^i, B_1^i), \dots, (A_{k^i}^i, B_{k^i}^i)$ will change whenever X crosses the boundary of a vistal cell. Local search can be formulated as the following convex optimization problem.

Objective

$$(1) \quad \min \quad F(X) = \sum_{i=1}^n \left(\sum_{l=1}^{k^i} (\|A_l^i\| + \|B_l^i\|)^2 + \sum_{e \in C^i} (|e|_X - |e|_{T^i})^2 \right)$$

Constraints

$$(2) \quad |e|_X \geq 0 \quad \forall e \in E$$

The minimizer of this optimization problem, X^* , satisfies $F(X^*) \leq F(X)$ for all X in $\mathcal{O}(E)$.

4.3. Optimality Qualifications. There are two cases for the optimal solution X^* : either every edge in X^* has a positive length or at least one edge in X^* does not. If every edge of X^* has positive length, then $X = X^*$ if and only if $\nabla F(X) = 0$ because the Fréchet function is continuously differentiable in the interior of $\mathcal{O}(E)$. The optimality condition for a point on a lower dimensional face of treespace can be expressed in terms of directional derivatives. In that case the optimality condition is

$$(3) \quad F'(X, Y) \geq 0 \quad \text{for all } Y \text{ such that } \mathcal{O}(X) \subseteq \mathcal{O}(Y)$$

By using Thm. 4.3 to separate the directional derivative into the contribution from the component of Y in $\mathcal{O}(X)$ and the component of Y which is perpendicular to $\mathcal{O}(X)$ the optimality condition can be expanded into a conditions on these independent terms,

and then simplified by taking advantage of the ability to express $F'(X, Y_X)$ in terms of the gradient of F at X relative to $\mathcal{O}(X)$. The following optimality conditions are expressed in terms of the Fréchet function (Def. 6.3) and the directional derivative of the Fréchet Function (Def. 4.1). Let $[\nabla F(X)]_e$ denote the partial derivative of the Fréchet function with respect to edge e , $\frac{\partial F(X)}{\partial e}$, which is well defined when $|e|_X > 0$.

- (4) $[\nabla F(X)]_e = 0$ for all $e : |e|_X > 0$
 (5) $F'(X, Y) \geq 0$ for all Y in $\mathcal{O}(E)$ such that the component of Y in $\mathcal{O}(X)$ is 0

The local search problem i.e. identifying the minimizer of the Fréchet function on an orthant of treespace, $\mathcal{O}(E)$, must have a unique solution because the Fréchet function is strictly convex and $\mathcal{O}(E)$ is a convex set. Also, optimality conditions for the local search problem are only different from global optimality conditions in one aspect, which is that rather than requiring $F'(X, Y) \geq 0$ for all Y perpendicular to $\mathcal{O}(X)$, it is only necessary to consider the subset of such points, Y , which are in $\mathcal{O}(E)$.

4.4. Verifying optimality. The focus of this section is developing an algorithm to answer the following question: Given a point X on a lower dimensional face of an orthant, $\mathcal{O}(E)$, does there exist Y such that $F'(X, Y) < 0$? To develop an algorithm to answer this question, the mathematical conditions of optimality from Sec. 4.3 are simplified into a collection of nested conditions.

The decomposed local optimality conditions, Cond. (4-5) state: partial derivatives with respect to positive length edges must be zero, and directional derivatives for directions which introduce new edges must be non-negative, respectively. Reformulating Cond. (5) as an optimization problem will lead to a simplified set of optimality conditions. Bounding the minimum directional derivative below by zero, as in the following optimization problem, is equivalent to bounding all directional derivatives below by zero.

$$(6) \quad f^* \geq 0,$$

where

$$(7) \quad f^* = \min_{\substack{Y \neq X \\ (Y - X) \perp \mathcal{O}(X)}} F'(X, Y)$$

The directional derivative of the Fréchet function, $F'(X, Y)$ is a positively homogeneous function. Since detecting a negative directional derivative is the goal, it is sufficient to bound the directional derivative below on the intersection of a sphere around X and the orthant $\mathcal{O}(E)$. Here we choose to restrict the search domain to the unit simplex around X . Restriction to this polyhedral set is advantageous because $F'(X, Y)$ is a convex function of Y , Lem. 6.10. Therefore, it is convex over a polyhedral subset of its domain. Let P be the vector of differences of edge lengths between Y and X with the component for edge e having value $p_e = |e|_Y - |e|_X$.

$$(8) \quad f_1^* = \min F'(X, Y)$$

$$(9) \quad \text{s.t.} \quad \sum_{e \in E} p_e = 1$$

$$(10) \quad p_e = 0 \text{ for all } e \text{ s.t. } |e|_X > 0$$

$$(11) \quad p_e \geq 0 \text{ for all } e \text{ s.t. } |e|_X = 0$$

The directional derivative is a once continuously differentiable function of Y with respect to edges such that $p_e > 0$. However, this is generally not the case when $p_e = 0$. Optimality qualifications for the optimization problem defining f_1^* need to account for non-differentiability. Thm. 4.4, in the same spirit as the Decomposition Theorem for Directional Derivatives,

Thm. 4.3, provides a decomposition for directional derivatives of directional derivatives. The directional derivative, $F'(X, Y)$, is a C^1 function of Y in $\mathcal{O}(Y)$, as shown in Lem. 6.11. Therefore, when the positive edge lengths of Y vary, the change in $F'(X, Y)$ can be quantified by partial derivatives of $F'(X, Y)$. The next theorem describes how the value of $F'(X, Y)$ changes in the case when lengths of edges in Y are increased from zero.

THEOREM 4.4. *Let X , Y , and Y' be three points in treespace such that X is a contraction of Y and Y is a contraction of Y' , that is $\mathcal{O}(X) \subset \mathcal{O}(Y) \subset \mathcal{O}(Y')$. Let $Y^\alpha = \Gamma(Y, Y'; \alpha)$. Let $Y'_{\perp \mathcal{O}(Y)}$ be the component of Y' which is perpendicular to the orthant containing Y , $\mathcal{O}(Y)$. When situated as described above, the directional derivative of the directional derivative, $F'(X, Y)$, when Y varies in the direction of Y' , that is*

$$(12) \quad \lim_{\alpha \rightarrow 0} \frac{F'(X, Y^\alpha) - F'(X, Y)}{\alpha},$$

is equal to the sum of a term contributed by changes which are parallel to the axes of $\mathcal{O}(Y)$ and the directional derivative of the Fréchet function at Y in the direction of $Y'_{\perp \mathcal{O}(Y)}$, $F'(Y, Y'_{\perp \mathcal{O}(Y)})$. The following expression gives a decomposition of the rate of change in the directional derivative into a term contributed from changing positive length edges, $|e|_Y > 0$ and a term contributed by increasing zero length edges, $|e|_Y = 0$. This decomposition is

$$(13) \quad \lim_{\alpha \rightarrow 0} \frac{F'(X, Y^\alpha) - F'(X, Y)}{\alpha} = \sum_{e \in E_Y} (|e|_{Y'} - |e|_Y) [\nabla F'(X, Y)]_e + F'(Y, Y'_{\perp \mathcal{O}(Y)}).$$

See Sec. 6 for proof.

With the decomposition from Thm. 4.4 one can express the optimality conditions for the optimization problem defined by (8-11) as follows. The optimal point Y^1 makes the vector of partial derivatives of the directional derivative, $\nabla_Y F'(X, Y)$, point away from the origin of the orthant and have a zero projection onto the set defined by $\sum_{e \in E} p_e = 1$. And, in any direction orthogonal to the orthant containing Y^1 the directional derivative from Y^1 is positive, that is $F'(Y^1, Y'_{\perp \mathcal{O}(Y^1)}) \geq 0$. Let $E^1 \subset E$ be the set of edges such that $|e|_{Y^1} - |e|_X > 0$. The optimality condition for a point X^* which minimizes the Fréchet function $F(X)$ in an orthant $\mathcal{O}(E)$ can be expanded to

$$(14) \quad \nabla F(X) = 0$$

$$(15) \quad F'(X, Y^1) \geq 0$$

$$(16) \quad \nabla_Y F'(X, Y^1) \perp \{Y \mid \sum_{e \in E^1} p_e = 1\}$$

$$(17) \quad F'(Y^1, Y) \geq 0 \text{ for all } Y \neq Y^1 \text{ s.t. } (Y - Y^1) \perp \mathcal{O}(Y^1).$$

This expanded optimality condition is obtained by reformulating a lower bound on the directional derivative of the Fréchet function as an optimization problem and applying the decomposition from Thm. 4.4. The same strategy can be applied first on the condition on line (17) and recursively on the resulting expansion. This strategy yields the following theorem.

THEOREM 4.5. *Consider trees Y^0, \dots, Y^k such that (i) $\mathcal{O}(Y^0) \subset \dots \subset \mathcal{O}(Y^k) = \mathcal{O}(E)$, and (ii) $Y^{i+1} - Y^i \perp \mathcal{O}(Y^i)$ for $i = 0, \dots, k-1$. Let E^i be the set of positive edges in Y^i for $i = 0, \dots, k$. Define a set of edge length difference vectors P^i for $i = 1, \dots, k$ with the component for edge e having value $p_e^i = |e|_{Y^i} - |e|_{Y^{i-1}}$. Denote the unit simplex in the orthant $\mathcal{O}(E^i \setminus E^{i-1})$ by $\Delta^i = \{P \in \mathcal{O}(E^i \setminus E^{i-1}) \mid \sum p_e^i = 1\}$. The minimizer of $F(X)$ in $\mathcal{O}(E)$ is Y^0 if and only if*

$$(18) \quad \nabla F(Y^0) = 0$$

$$(19) \quad F'(Y^{i-1}, Y^i) \geq 0 \text{ for } i = 1, \dots, k$$

$$(20) \quad \nabla F'(Y^{i-1}, Y^i) \perp \Delta^i \text{ for } i = 1, \dots, k.$$

See Sec. 6 for proof.

5. Methods for optimizing edge lengths. This section contains the fundamentals for an iterative local search algorithm: initialization, an improvement method, and a method to verify optimality.

5.1. A damped Newton's method. Alg. 1 is designed to find approximately optimal edge lengths for a fixed tree topology. Detailed explanations for the steps of this algorithm are in the following subsections.

δ - ϵ optimality conditions

Conditions for a point X on the interior of an orthant to be approximately optimal are:

$$(21) \quad [\nabla F(X)]_e \geq 0 \quad \text{or} \quad \begin{cases} |[\nabla F(X)]_e| < \delta & \text{for all } e : |e|_X > \epsilon \\ |[\nabla F(X)]_e| < \delta & \text{for all } e : |e|_X < \epsilon \end{cases}$$

If the δ - ϵ optimality conditions are satisfied then $F(X^*)$ will not differ much from the Fréchet function value when the lengths of edges with positive derivatives are set to 0.

Algorithm 1 Interior point algorithm for optimal edge lengths

input: $T^1, T^2, \dots, T^n, X^0 \in \mathcal{T}_r$, $\epsilon > 0$, $\delta > 0$, $0 < c < 1$
while δ - ϵ optimality conditions (21) are not satisfied **do**
 compute a descent direction P (Sec. 5.1.1)
 find a feasible step-length, α , satisfying decrease condition (Sec. 5.1.2)
 let $X^{k+1} = X^k + \alpha P$
 if $|e| < \epsilon$ **then** remove edge e from tree X
end while

5.1.1. Newton steps. A successful iterative algorithm will make substantial progress to an optimal point. This can be achieved using a modified Newton's method. Newton's method uses a descent vector which points to the minimizer of a quadratic approximation of the objective function. The quadratic approximation in Newton's method uses the first three terms of the Taylor expansion of $F(X)$. For the Fréchet function the entries of the Hessian matrix of second order partial derivatives is given in Def. 6.4.

The Hessian matrix is positive definite because the Fréchet function is strictly convex. Let $[\nabla^2 F(X)]_{ee'} = \frac{\partial^2 F(X)}{\partial e \partial e'}$, which is well defined when $|e|_X > 0$ and $|e'|_X > 0$. When the Hessian and gradient are well defined, the second order Taylor approximation is

$$(22) \quad g(X; p) = F(X) + \sum_{e \in E} p_e [\nabla F(X)]_e + \sum_{e \in E} \sum_{e' \in E} p_e p_{e'} [\nabla^2 F(X)]_{ee'}.$$

The minimizer in p of $g(X; p)$ is the Newton vector $p^N = -\nabla F(X)(\nabla^2 F(X))^{-1}$.

5.1.2. Choosing a step length. Taking a full step along the Newton direction minimizes the quadratic approximation of the Fréchet function. However, taking a full step may result in a new point which actually has a larger Fréchet function value or that may be beyond orthant boundaries.

The first precaution is to calculate the maximum step length α_0 such that $|e|_{k+1} = |e|_k + \alpha_0 p_e \geq 0$ for all e . If $\alpha_0 \leq 1$ then let $\alpha = \alpha_0 c_0$ where $0 < c_0 < 1$.

Choosing step-length which satisfies the following *sufficient decrease condition* will ensure a substantial decrease in the objective function value at every step. Let $0 < c_1 < 1$.

$$(23) \quad F(X^k + \alpha p) \leq F(X^k) + c_1 \alpha \sum_{e \in E_{X^k}} [\nabla F(X)]_e p_e$$

The *curvature condition*, which rules out unacceptably short steps, requires the step-length, α , to satisfy

$$(24) \quad \sum_{e \in E_{X^k}} [\nabla F(X^k + \alpha p)]_e p_e \geq c_2 \sum_{e \in E_{X^k}} [\nabla F(X)]_e p_e$$

for some constant c_2 in the interval $(c_1, 1)$.

5.1.3. Initialization. For initializing an interior point search, any point in $\mathcal{O}(E)$ would suffice, but it is preferential to start with a good guess for edge lengths. The global search algorithms presented in [17, 2, 3] could provide a starting point for a local search. One good start strategy can be derived by noticing that the Fréchet function can be separated into a quadratic part and a part involving sums of norms.

$$(25) \quad F(X) = \sum_{i=1}^n \sum_{l=1}^{k^i} \|A_l^i\|^2 + 2\|A_l^i\| \|B_l^i\| + \|B_l^i\|^2 + \sum_{e \in C^i} (|e|_X^2 - |e|_{T^i})^2$$

The only terms that cannot be expressed in a quadratic function of the edge lengths are collected into function

$$(26) \quad S(X) = \sum_{i=1}^n \sum_{l=1}^{k^i} 2\|A_l^i\| \|B_l^i\|$$

Subtracting $S(X)$ from $F(X)$ yields a quadratic function,

$$(27) \quad Q(X) = F(X) - S(X) = \sum_{i=1}^n \sum_{l=1}^{k^i} \|A_l^i\|^2 + \|B_l^i\|^2 + \sum_{e \in C^i} (|e|_X - |e|_{T^i})^2,$$

The minimizer of $Q(X)$, X_Q^* , can be easily found by solving $\nabla Q(X) = 0$; the solution is

$$(28) \quad |e|_{X_Q^*} = \frac{\sum_{i=1}^n |e|_{T^i}}{n}.$$

The optimal value $|e|_{X_Q^*}$ is non-negative, and if e has a positive length in any of T^1, \dots, T^n , then $|e|_{X_Q^*}$ is positive.

The gradient of $S(X)$ is non-negative at any feasible X . Therefore, at any X such that $\nabla Q(X) = 0$, the gradient of the Fréchet function is greater than or equal to zero at every coordinate, $\nabla F(X) = \nabla Q(X) + \nabla S(X) \geq 0$. Which implies that the optimal edge lengths in X^* must be no larger than the edge lengths in X_Q^* i.e. the optimal solution is in the closed box

$$(29) \quad 0 \leq |e|_X \leq |e|_{X_Q^*} \quad \forall e \in E.$$

Thus a reasonable starting point for search inside orthant $\mathcal{O}(E)$ would be X_Q^* , or any point strictly inside the box defined by Eq. (29).

5.2. Iterative algorithm for verifying optimality in a closed orthant. The optimality condition in Thm. 4.5 is the logical basis for the Alg.2, which finds the minimizer of the Fréchet function $F(X)$ in the closure of a fixed orthant, $\mathcal{O}(E)$.

6. Differential analysis of the Fréchet function in treespace. Analysis of how $F(X)$ changes with respect to X provides useful insights for designing fast optimization algorithms. This analysis is aimed at providing summaries for how the value of $F(X)$ changes with respect to X .

The results in this section are summarized as follows: Cor. 6.2 gives the value of the directional derivative when $\mathcal{O}(X) = \mathcal{O}(Y)$ and Thm. 6.6 gives the value of the directional derivative when $\mathcal{O}(X) \subseteq \mathcal{O}(Y)$, when assuming Y is contained in the interior of a multi-vistal facet. In Lem. 6.7 we show that when Y is on a multi-vistal face the value of the directional derivative can be expressed equivalently using any of the representations for the geodesics from T^1, \dots, T^n to Y . In Lem. 6.8 and Lem. 6.10 we show that the directional derivative is continuous and convex with respect to Y when $\mathcal{O}(X) \subseteq \mathcal{O}(Y)$. The proofs of Thm. 4.3, 4.4, and 4.5 are presented at the end of Sec. 6.

Algorithm 2 Algorithm to minimize Fréchet sum of squares in orthant $\mathcal{O}(E)$

input: $E; T^1, T^2, \dots, T^n; \epsilon, \delta > 0$
initialize: $i, k = 1; E^0 = \text{optimal star tree}; E^1 = E \setminus \{\text{leaf edges}\}; \epsilon^0, \epsilon^1 = \epsilon$
while $i \geq 1$ **do**
 Find $Y^* \in \mathcal{O}(E^i)$ which approx. minimizes $F'(Y^{i-1}, Y)$,
 where $Y - Y^{i-1}$ is orthogonal to $\mathcal{O}(E^0 \cup \dots \cup E^{i-1})$
 while approx. optimality conditions with ϵ^i and δ are not satisfied **do**
 damped Newton
 end while
 if there are some zero length edges, S
 $(E, Y, \epsilon)^{i+1} = (E, Y, \epsilon)^i, \dots, (E, Y, \epsilon)^{k+1} = (E, Y, \epsilon)^k; k = k + 1$
 $E^i = E^i \setminus S; |e|_{Y^i} = 0 \text{ if } e \in S$
 $i = i + 1$
 else
 if $F'(Y^{i-1}, Y^*) < 0$
 find step size α , along $\Gamma(Y^{i-1}, Y^*)$;
 $E^{i-1} = E^{i-1} \cup E^i; Y^{i-1} = Y^{i-1} + \alpha Y^*; \epsilon^{i-1} = \alpha \epsilon$ where $0 < \alpha < 1$;
 $(E, Y, \epsilon)^i = \emptyset; (E, Y, \epsilon)^i = (E, Y, \epsilon)^{i+1}, \dots, (E, Y, \epsilon)^{k-1} = (E, Y, \epsilon)^k$
 $i = i - 1, k = k - 1$
 else
 $i = i - 1$
 end if
 end if
end while
Find the minimizer of $F(X)$ in $\mathcal{O}(E^0)$.

When both X and Y are in the relative interior of the same maximal orthant of treespace, where the gradient at X is well defined in $\mathcal{O}(Y)$, the directional derivative can be expressed in terms of the gradient at X inside $\mathcal{O}(Y)$. However when $\mathcal{O}(X) \subset \mathcal{O}(Y)$, the gradient at X is not well defined in $\mathcal{O}(Y)$. Analysis of the directional derivative in the later situation, which is one of the main focuses of this section, is important because it facilitates concise specification of optimality conditions and an efficient algorithm for verifying that a point on a lower dimensional face of an orthant \mathcal{O} is the minimizer of the Fréchet function within \mathcal{O} .

THEOREM 6.1. [17, Cor. 4.1] *The gradient of F is well defined on the interior of every maximal orthant \mathcal{O} .*

Idea of proof. The Fréchet function is smooth in each multi-vistal facet, and it can be shown that the gradient function has the same value in every multi-vistal facet containing X in the interior of \mathcal{O} . Therefore the gradient is well-defined on the interior of \mathcal{O} .

COROLLARY 6.2. *When X and Y are in the same maximal orthant the value of directional derivative from X to Y can be expressed in terms of the gradient at X , and the differences in edge lengths $p_e = |e|_Y - |e|_X$, as*

$$(30) \quad F'(X, Y) = \sum_{e \in E_X} p_e [\nabla F(X)]_e$$

Proof. Expression of a directional derivative of a smooth function in terms of its gradient is a standard technique in calculus. \square

The gradient may not be well-defined on a lower-dimensional orthant of treespace. For a point on a lower dimensional orthant of treespace, a well-defined analogue to the gradient is the *restricted gradient*.

DEFINITION 6.3. *Let $(A_1^i, B_1^i), \dots, (A_{k^i}^i, B_{k^i}^i)$ be a support sequence for the geodesic from X to T^i . The restricted gradient is the vector of partial derivatives which correspond to*

points Y with $\mathcal{O}(X) \subseteq \mathcal{O}(Y)$ and $Y - X$ parallel to the axes of $\mathcal{O}(X)$. If $|e|_X > 0$ then

$$(31) \quad [\nabla F(X)]_e = \frac{\partial F(X)}{\partial e}$$

$$(32) \quad = \lim_{\Delta e \rightarrow 0} \frac{F(X + \Delta e) - F(X)}{\Delta e}$$

$$(33) \quad = \sum_{i=1}^n \begin{cases} |e|_X \left(1 + \frac{\|B_l^i\|}{\|A_l^i\|}\right) & \text{if } e \in A_l^i \\ (|e|_X - |e|_{T^i}) & \text{if } e \in C^i \end{cases}$$

and if $|e|_X = 0$ then $[\nabla F(X)]_e = 0$.

When X is on the interior of a maximal orthant of treespace then the restricted gradient is the same as the gradient. Note that in the case when $A_l^i = \{e\}$, $|e|_X \left(1 + \frac{\|B_l^i\|}{\|A_l^i\|}\right) = |e|_X + \|B_l^i\|$.

Second order derivatives will be used in calculating Newton directions in Sec. 5.

DEFINITION 6.4. *Let X be a point in the interior of a multi-vistal cell relative to an orthant of treespace, \mathcal{O} . The restricted Hessian on \mathcal{O} is the matrix of second order partial derivatives with entries having the following values:*

$$(34) \quad [\nabla^2 F(X)]_{ef} = 2 \sum_{i=1}^r \begin{cases} 1 + \frac{\|B_l^i\|}{\|A_l^i\|} - \frac{\|B_l^i\|}{\|A_l^i\|^3} x_e^2 & \text{if } e = f, e \in A_l^i, |A_l^i| > 1 \\ 1 & \text{if } e = f, e \in A_l^i, A_l^i = \{e\} \\ 1 & \text{if } e = f, e \in C^i \\ -\frac{\|B_l^i\|}{\|A_l^i\|^3} x_e x_f & \text{if } e \neq f, e, f \in A_l^i \\ 0 & \text{otherwise} \end{cases}$$

If either $|e|_X = 0$ or $|f|_X = 0$ then $[\nabla^2 F(X)]_{ef} = 0$.

THEOREM 6.5. *The value of the restricted gradient at a point X can be expressed equivalently using the algebraic form of the Fréchet function from any of the multi-vistal facets containing X .*

Proof. The restricted gradient has the same value using any of the valid support sequences defined by vistal cells on the relative interior of \mathcal{O} .

We now verify that at X the gradient of $d^2(X, T^i)$ is the same for every valid support and signature. The gradient of $d^2(X, T^i)$ for the support $(\mathcal{A}, \mathcal{B})$ is given as follows. Let the variable length of edge e in X be written as x_e .

$$(35) \quad \frac{\partial d^2(X, T^i)}{\partial x_e} = \begin{cases} 2 \left(1 + \frac{\|B_j^i\|}{\|A_j^i\|}\right) x_e & \text{if } e \in A_j^i \\ 2(x_e - |e|_{T^i}) & \text{if } e \in C^i \end{cases}$$

In this paragraph we focus on the behavior of the geodesic, Γ^i , from X to tree, T^i . We drop the superscript i to make the notation less cumbersome when comparing two valid supports for the same geodesic. The geodesic Γ has a unique support $(\mathcal{A}, \mathcal{B})$ satisfying (P3) with strict inequalities,

$$(36) \quad \frac{\|A_1\|}{\|B_1\|} < \frac{\|A_2\|}{\|B_2\|} < \dots < \frac{\|A_k\|}{\|B_k\|}.$$

From [17, Sec. 3.2.2], any other support $(\mathcal{A}', \mathcal{B}')$ for Γ must have a signature \mathcal{S}' in (P3) with some equality subsequences. Suppose that A'_j and B'_j are in some equality subsequence satisfying (P2) with B'_j containing the edge e . Then for the support pair A_i and B_i such that B_i contains e , it must hold that $\frac{\|A'_j\|}{\|B'_j\|} = \frac{\|A_i\|}{\|B_i\|}$. Now we can see that $\left(1 + \frac{\|B'_j\|}{\|A'_j\|}\right) x_e = \left(1 + \frac{\|B_i\|}{\|A_i\|}\right) x_e$, and that the gradient of $d^2(X, T^i)$ is the same on every multi-vistal facet containing X on the relative interior of \mathcal{O} . \square

Now we extend the results for directional derivatives to the situation when $\mathcal{O}(X) \subset \mathcal{O}(Y)$.

THEOREM 6.6. *Suppose that Y lies in the interior of multi-vistal facet V_Y , and X is some point in V_Y . Let $(A_1^i, B_1^i), \dots, (A_m^i, B_m^i)$ be the support pairs for the geodesic from Y to T^i and let C^i be the set of edges in Y which are common in T^i . Let E_X be the set of edges with positive lengths in X . Let P be the vector with components $p_e = |e|_Y - |e|_X$ so that $\Gamma(X, Y; \alpha) = X + \alpha P$, and let $Z_\alpha := \Gamma(X, Y; \alpha)$. Then the value of directional derivative from X to Y is*

$$F'(X, Y) = \sum_{e \in E_X} p_e [\nabla F(X)]_e + 2 \sum_{i=1}^n \left(\sum_{l: \|A_l^i\|_X = 0} (\|A_l^i\|_P \|B_l^i\|_{T^i}) - \sum_{e \in C^i \setminus E_X} p_e |e|_{T^i} \right).$$

Where $\|A\|_X$, means use the edge length mapping from tree X in evaluating the norm of the set of edges A , that is $\|A\|_X = \sqrt{\sum_{e \in A} |e|_X^2}$.

Proof. Let Z_α be a point on the geodesic segment between X and Y . The length of edge e in Z_α be $|e|_Z = |e|_X + \alpha p_e$. The Fréchet function is the sum of squared distances from a variable point to each of the data points T^1, \dots, T^n , so the directional derivative of the Fréchet function is the sum over the indexes of the data points of the directional derivatives of the square distances.

$$(37) \quad F'(X, Y) = \lim_{\alpha \rightarrow 0} \frac{F(Z_\alpha) - F(X)}{\alpha}$$

$$(38) \quad = \lim_{\alpha \rightarrow 0} \frac{\sum_{i=1}^n d^2(Z_\alpha, T^i) - \sum_{i=1}^n d^2(X, T^i)}{\alpha}$$

$$(39) \quad = \sum_{i=1}^n \left(\lim_{\alpha \rightarrow 0} \frac{d^2(Z_\alpha, T^i) - d^2(X, T^i)}{\alpha} \right)$$

For a set of edges A , let $\|A\|_X = \sqrt{\sum_{e \in A} |e|_X^2}$. If an edge e has zero length in a tree, X , or is compatible with X but not present then take $|e|_X$ to be 0. The squared distance from Z_α to T^i can be expressed as

$$(40) \quad d^2(Z_\alpha, T^i) = \sum_{l=1}^{k^i} (\|A_l^i\|_{Z_\alpha} + \|B_l^i\|)^2 + \sum_{e \in C^i} (|e|_{Z_\alpha} - |e|_{T^i})^2$$

The squared distance has three types of terms: a term representing the contribution from common edges, terms for support pairs with $\|A_l^i\|_X > 0$, and terms for support pairs with $\|A_l^i\|_X = 0$. In the first two cases the gradient is well-defined, and taking the inner-product of the directional vector and the gradient will yield their contributions to the directional derivative. In the third case the gradient is undefined, and its value will be obtained by analyzing the limit directly as follows.

$$(41) \quad \left(\lim_{\alpha \rightarrow 0} \frac{\sum_{l=1}^{k^i} (\|A_l^i\|_{Z_\alpha} + \|B_l^i\|)^2 - \sum_{l=1}^{k^i} (\|A_l^i\|_X + \|B_l^i\|)^2}{\alpha} \right)$$

Bringing out the sum and canceling in the numerators yields,

$$(42) \quad \sum_{l=1}^{k^i} \lim_{\alpha \rightarrow 0} \frac{\|A_l^i\|_Z^2 - \|A_l^i\|_X^2 + 2\|B_l^i\| (\|A_l^i\|_Z - \|A_l^i\|_X)}{\alpha}$$

The limit of the fraction can be split into the sum of two limits,

$$(43) \quad \lim_{\alpha \rightarrow 0} \frac{\|A_l^i\|_Z^2 - \|A_l^i\|_X^2 + 2\|B_l^i\| (\|A_l^i\|_Z - \|A_l^i\|_X)}{\alpha}$$

$$(44) \quad = \lim_{\alpha \rightarrow 0} \frac{\|A_l^i\|_Z^2 - \|A_l^i\|_X^2}{\alpha} + \lim_{\alpha \rightarrow 0} \frac{2\|B_l^i\| (\|A_l^i\|_Z - \|A_l^i\|_X)}{\alpha}$$

If every edge in A_l^i has length zero in X , and thus $\|A_l^i\|_X = 0$, the limit on the left is 0 and the limit on the right simplifies to

$$(45) \quad 2\|B_l^i\|\|A_l^i\|_P$$

The partial derivative of the squared distance from X to T^i with respect to the length of edge e , that is the component for edge e in the restricted gradient vector, is

$$(46) \quad [\nabla d^2(X, T^i)]_e = \begin{cases} |e|_X \left(1 + \frac{\|B_l^i\|}{\|A_l^i\|}\right) & \text{if } e \in A_l^i \\ (|e|_X - |e|_{T^i}) & \text{if } e \in C^i \end{cases}$$

The directional derivative of the squared distance simplifies to

$$(47) \quad \lim_{\alpha \rightarrow 0} \frac{d^2(Z, T^i) - d^2(X, T^i)}{\alpha}$$

$$(48) \quad = \sum_{e \in E_X} p_e [\nabla d^2(X, T^i)]_e + 2 \sum_{l: \|A_l^i\|_X = 0} \left(\|B_l^i\| \sqrt{\sum_{e \in A_l^i} p_e^2} \right) - 2 \sum_{e \in C^i \setminus E_X} p_e |e|_{T^i}$$

Summing the directional derivatives of the squared distances over T^1, \dots, T^n yields the expression for the value of the directional derivative in the theorem. \square

Each tree T^i induces pre-vistal facets on treespace and taken together the collection subdivides treespace into pre-multi-vistal facets where the Fréchet function can be represented in a fixed form. On the shared faces of pre-vistal facets the Fréchet function can be represented in multiple valid forms. At such points the value of the Fréchet function and gradient are the same, but higher order derivatives can differ depending on which representation of the Fréchet function is used. In the following lemma the directional derivative is determined to be well-defined at such points. We now extend the results to the situation where Y is allowed to be on a vistal face. In this situation there can be multiple valid support sequences for the geodesics from Y to T^1, \dots, T^n .

LEMMA 6.7. *Suppose that X and Y are in the same multi-vistal facet, \mathcal{V} , and that Y is on a face of \mathcal{V} on the interior of an orthant. The value of the directional derivative can be expressed equivalently using any valid support sequences for the geodesics from Y to T^1, \dots, T^n .*

Proof. The form of $F'(X, Y)$ is constant within an open multi-vistal facet, and changes at boundaries of vistal facets. When Y reaches the boundary of a vistal facet, that is either at least one of the (P2) constraints reaches equality, at least one of the (P3) constraints reaches equality, or when the length of an edge reaches zero or increases from zero, this is called the collision of Y with the boundary of that vistal facet. A point T^i , and associated geodesic $\Gamma(T^i, Y)$ are said to generate the vistal facet collision. When Y collides with a (P2) boundary of a vistal facet at least two support pairs for the geodesic merge; and when Y collides with a (P3) boundary at least two support pairs for the geodesic could be split in such a way that the resulting support is valid. In either case there are at least two valid forms for the geodesic. Let $(C_1, D_1), (C_2, D_2)$ be support pairs which are formed from a partition of the support pair (A_l^i, B_l^i) , such that either of the following support sequences for the geodesic from Y to T^i is valid: $(A_1^i, B_1^i), \dots, (A_l^i, B_l^i), \dots, (A_m^i, B_m^i)$ or $(A_l^i, B_l^i), \dots, (C_1, D_1), (C_2, D_2), \dots, (A_m^i, B_m^i)$; and $\frac{\|C_1\|}{\|D_1\|} = \frac{\|C_2\|}{\|D_2\|} = \frac{\|A_l^i\|}{\|B_l^i\|}$. Rescaling the lengths of edges in A_l^i does not change the form of the geodesic for small α and $l \leq k$. Parameterizing the lengths of edges in terms of α and canceling α yields $\frac{\sqrt{\sum_{e \in C_1} p_e^2}}{\|D_1\|} = \frac{\sqrt{\sum_{e \in C_2} p_e^2}}{\|D_2\|} = \frac{\sqrt{\sum_{e \in A_l^i} p_e^2}}{\|B_l^i\|}$. That fact, and the fact that $C_1 \cup C_2$ partition A_l^i , and $D_1 \cup D_2$ partition B_l^i implies that $\|D_1\| \sqrt{\sum_{e \in C_1} p_e^2} + \|D_2\| \sqrt{\sum_{e \in C_2} p_e^2} = \|B_l^i\| \sqrt{\sum_{e \in A_l^i} p_e^2}$. Thus

the directional derivative is continuous across vial facet boundaries from (P2) and (P3) constraints. \square

Now we extend the results for directional derivatives to directions issuing from X to points Y in a small enough radius such that $\mathcal{O}(X) \subseteq \mathcal{O}(Y)$ and X and Y share a multi-vial facet.

LEMMA 6.8. *The directional derivative, $F'(X, Y)$, is a continuous function of Y over the set of Y such that $\mathcal{O}(X) \subseteq \mathcal{O}(Y)$ and X and Y share a vial facet.*

Proof. The directional derivative is a continuous function at the faces of orthants because when an edge length $|e|_Y$ increases from zero its contribution to $F'(X, Y)$ is a continuous function which starts at the value zero. Thus, when the topology of Y changes $F'(X, Y)$ changes continuously as a function of the edge lengths. \square

The following lemma is used in the proof of Lem. 6.10, and was also discovered independently by Megan Owen [18].

LEMMA 6.9. *Let Y^0 and Y^1 be points in \mathcal{T}_r such that $\mathcal{O}(X) \subseteq \mathcal{O}(Y^0)$ and $\mathcal{O}(X) \subseteq \mathcal{O}(Y^1)$. Let $Y^t = \Gamma(Y^0, Y^1; t)$ be the point which is proportion t along the geodesic from Y^0 to Y^1 . The point which is α proportion along the geodesic from X to Y^t is t proportion along the geodesic between the point $\Gamma_{X, Y^0}(\alpha)$ and the point $\Gamma_{X, Y^1}(\alpha)$, that is $\Gamma(X, Y^t; \alpha) = \Gamma(\Gamma(X, Y^0; \alpha), \Gamma(X, Y^1; \alpha); t)$.*

Proof. Let $Y^0(\alpha) = \Gamma_{X, Y^0}(\alpha)$ and let $Y^1(\alpha) = \Gamma_{X, Y^1}(\alpha)$. Let $C = E_{Y^0(\alpha)} \cap E_{Y^1(\alpha)}$. By definition $E_X \subseteq C$. The length of e in $Y^0(\alpha)$ is

$$(49) \quad |e|_{Y^0(\alpha)} = \begin{cases} |e|_X + \alpha |e|_{Y^0} & \text{if } e \in C \\ \alpha |e|_{Y^0} & \text{if } e \in E_{Y^0} \setminus C \end{cases}$$

and the length of e in $Y^1(\alpha)$ is

$$(50) \quad |e|_{Y^1(\alpha)} = \begin{cases} |e|_X + \alpha |e|_{Y^1} & \text{if } e \in C \\ \alpha |e|_{Y^1} & \text{if } e \in E_{Y^1} \setminus C \end{cases}$$

A geodesic support sequence which is valid for the geodesic between Y^0 and Y^1 is valid for the geodesic between $Y^0(\alpha)$ and $Y^1(\alpha)$. The incompatibilities of edges in A and B are the same for any α . Suppose that a support sequence satisfies (P2) and (P3) for some α . Factoring out α from the numerators and denominators of the (P2) and (P3) ratios reveals that the combinatorics of the geodesic between $Y^0(\alpha)$ and $Y^1(\alpha)$ depends on the relative proportions of lengths of edges in Y^0 and Y^1 , and not on the value of α . That is,

$$(51) \quad \frac{\|A_l\|_{Y^0(\alpha)}}{\|B_l\|_{Y^1(\alpha)}} = \frac{\sqrt{\sum_{e \in A_l} \alpha |e|_{Y^0}}}{\sqrt{\sum_{e \in B_l} \alpha |e|_{Y^1}}} = \frac{\|A_l\|_{Y^0}}{\|B_l\|_{Y^1}}$$

Now we show that $|e|_{\Gamma_{Y^0(\alpha)Y^1(\alpha)}(t)} = |e|_{\Gamma_{XY^t}(\alpha)}$. The combinatorics of the geodesic between $Y^0(\alpha)$ and $Y^1(\alpha)$ do not depend on α . Therefore, which edges have positive lengths in the l^{th} leg of $\Gamma_{Y^0(\alpha)Y^1(\alpha)}$ does not depend on α . The length of edge e at $\Gamma_{Y^0(\alpha)Y^1(\alpha)}(t)$ is

$$(52) \quad |e|_{\Gamma_{Y^0(\alpha)Y^1(\alpha)}(t)} = \begin{cases} \frac{(1-t)\|A_j\|_{\alpha-t\|B_j\|_{\alpha}}}{\|A_j\|_{\alpha}} |e|_{Y^0(\alpha)} & e \in A_j \\ \frac{t\|B_j\|_{\alpha} - (1-t)\|A_j\|_{\alpha}}{\|B_j\|_{\alpha}} |e|_{Y^1(\alpha)} & e \in B_j \\ (1-t)|e|_{Y^0(\alpha)} + t|e|_{Y^1(\alpha)} & e \in C \end{cases}$$

(53)

Substituting $\|A_j\|_\alpha = \alpha\|A_j\|$, $\|B_j\|_\alpha = \alpha\|B_j\|$, 49, and 50 yields

$$(54) \quad |e|_{\Gamma_{Y^0(\alpha)Y^1(\alpha)}(t)} = \begin{cases} \alpha \frac{(1-t)\|A_j\| - t\|B_j\|}{\|A_j\|} |e|_{Y^0} & e \in A_j \\ \alpha \frac{t\|B_j\| - (1-t)\|A_j\|}{\|B_j\|} |e|_{Y^1} & e \in B_j \\ |e|_X + \alpha((1-t)|e|_{Y^0} + t|e|_{Y^1}) & e \in C \end{cases}.$$

Now the length of e in $\Gamma_{XY^t}(\alpha)$ is

$$(55) \quad |e|_{\Gamma_{XY^t}(\alpha)} = \begin{cases} |e|_X + \alpha|e|_{Y^t} & \text{if } e \in C \\ \alpha|e|_{Y^t} & \text{if } e \in E_{Y^t} \setminus C \end{cases}$$

The length of e in Y^t is given by

$$(56) \quad |e|_{Y^t} = \begin{cases} \frac{(1-t)\|A_j\| - t\|B_j\|}{\|A_j\|} |e|_{Y^0} & e \in A_j \\ \frac{t\|B_j\| - (1-t)\|A_j\|}{\|B_j\|} |e|_{Y^1} & e \in B_j \\ ((1-t)|e|_{Y^0} + t|e|_{Y^1}) & e \in C \end{cases}.$$

Therefore $|e|_{\Gamma_{Y^0(\alpha)Y^1(\alpha)}(t)} = |e|_{\Gamma_{XY^t}(\alpha)}$ holds. \square

LEMMA 6.10. *The directional derivative $F'(X, Y)$ is a convex function of Y over the set of Y such that $\mathcal{O}(X) \subseteq \mathcal{O}(Y)$ and X and Y share a vial facet.*

Proof. Let Y^0 and Y^1 be points in \mathcal{T}_r such that $\mathcal{O}(X) \subseteq \mathcal{O}(Y^0)$ and $\mathcal{O}(X) \subseteq \mathcal{O}(Y^1)$. Let Y^t be the point which is proportion t along the geodesic from Y^0 to Y^1 . Let $\Gamma_{XY^t}(\alpha) : [0, 1] \rightarrow \mathcal{T}_r$ be a function which parameterizes the geodesic from X to Y^t . Using Lem. 6.9 and the strict convexity of F together yields

$$(57) \quad F(\Gamma_{XY^t}(\alpha)) < F(\Gamma_{XY^0}(\alpha))(1-t) + F(\Gamma_{XY^1}(\alpha))t$$

The directional derivative from X in the direction of $\Gamma_{XY^t}(\alpha)$ is

$$(58) \quad F'(X, Y^t) = \lim_{\alpha \rightarrow 0} \frac{F(\Gamma_{XY^t}(\alpha)) - F(X)}{\alpha}$$

Substituting for $F(\Gamma_{XY^t}(\alpha))$ using the inequality on line (57) yields,

$$(59) \quad F'(X, Y^t) \leq \lim_{\alpha \rightarrow 0} \frac{F(\Gamma_{XY^0}(\alpha))(1-t) + F(\Gamma_{XY^1}(\alpha))t - F(X)}{\alpha}$$

Note that strict inequality may not hold even though the Fréchet function is convex because in the limit the value may approach an infimum. Simplifying by separating the fraction and limit reveals that the directional derivative is convex in Y ,

$$(60) \quad F'(X, Y^t) \leq (1-t) \lim_{\alpha \rightarrow 0} \frac{F(\Gamma_{XY^0}(\alpha)) - F(X)}{\alpha} + t \lim_{\alpha \rightarrow 0} \frac{F(\Gamma_{XY^1}(\alpha)) - F(X)}{\alpha}$$

$$(61) \quad = (1-t)F'(X, Y^0) + tF'(X, Y^1) \quad \square$$

LEMMA 6.11. *Let X and Y be points such that $\mathcal{O}(X) \subseteq \mathcal{O}(Y)$. $F'(X, Y)$ is a C^1 function of Y on the interior of the orthant $\mathcal{O}(Y)$.*

Proof. Within any fixed multi-vistal face the algebraic form of F is a sum of smooth functions, and the restricted gradient function is continuous at the boundaries of multi-vistal faces relative to the interior of $\mathcal{O}(Y)$. \square

Let X and Y be points in \mathcal{T}_r such that X and Y share a pre-multi-vistal facet defined by geodesics from X to T^1, \dots, T^n . If this is the case, then either (i) X and Y have the same topology, (ii) X is a contraction of Y or (iii) Y is a contraction of X . Assume that if the topologies of trees X and Y differ then X is a contraction of Y , that is $\mathcal{O}(X) \subseteq \mathcal{O}(Y)$. Let $\Gamma(X, Y; \alpha)$, where $0 \leq \alpha \leq 1$, be the point α proportion along the geodesic from X to Y . In the limit as α approaches 0, the behavior of support pairs from X to T is pivotal in understanding the behavior of the Fréchet function on faces of orthants. In particular, it is important to distinguish those support pairs which do not exist at a point X on the face of $\mathcal{O}(Y)$.

DEFINITION 6.12. *Let $(A_1, B_1), \dots, (A_k, B_k)$ be a support sequence for the geodesic from Y to a tree T , as in the definition of directional derivative above, Def. 4.1. Let any support pair (A_l, B_l) such that $\|A_l\|_X = 0$ be called a local support pair.*

Local support pairs will be the earliest support pairs in a support sequence for the geodesic between Y and T . Y and X share a vistal facet, that is their geodesics to T can be represented with the same support sequence. According to (P2), any support pair such that $\|A_l\|_X = 0$ must be among the first support pairs in the support sequence. Thus, let $(A_1, B_1), \dots, (A_m, B_m)$ be local support pairs, and let $(A_{m+1}, B_{m+1}), \dots, (A_k, B_k)$ be the rest of the geodesic support sequence being used to represent the geodesic between Y and T .

Let \tilde{B} be all edges from T which are incompatible with at least one edge in Y but not incompatible with any edge in X and let \tilde{A} be all edges from Y which are incompatible with some edge in \tilde{B} .

LEMMA 6.13. *Any sequence of local support pairs, $(A_1, B_1), \dots, (A_m, B_m)$ have the property that the sets A_1, \dots, A_m partition \tilde{A} and B_1, \dots, B_m partition \tilde{B} .*

Proof. Any edge in T which is incompatible with an edge in a local support pair, (A_l, B_l) is compatible with every edge in X because for a local support pair $\|A_l\|_X = 0$. Therefore any edge from T in a local support pair must be in \tilde{B} .

An edge in \tilde{B} is compatible with every edge in X . Therefore, such an edge cannot be in any of the support pairs with edges from X , and thus must be in a local support pair.

Suppose an edge, e , from Y is in a local support pair, (A_l, B_l) , then it must be incompatible with at least one edge in T . All the edges which are in B_l must be compatible with all edges in X because $\|A_l\|_X = 0$. Since e is incompatible with some edge in T that is not incompatible with any edge in X , e must be in \tilde{A} .

Let e be an edge in \tilde{A} . Edge e is not in X , and edge e is incompatible with at least one edge in T which no edge in X is incompatible with. Edge e must be in a support pair so that along the geodesic the length of e contracts to zero before all the edges in \tilde{B} can switch on. Therefore e must be a support pair with at least one of the edges in \tilde{B} that it is incompatible with. Since all edges in \tilde{B} are in local support pairs, all edges in \tilde{A} must also be in local support pairs. \square

COROLLARY 6.14. *Any sequence of local support pairs which is valid for the geodesic from Y to T is also valid for the geodesic from Y_\perp to T and vice versa.*

Proof. Lem. 6.13 implies local support pairs for the geodesic from Y to T and Y_\perp to T would be composed from the same sets of edges. Factoring out α , we see that the relative lengths of edges in \tilde{A} are the same in Y and Y_\perp . \square

Proof of Thm. 4.3

Proof. Note that since X and Y are in the same orthant, the geodesic Γ_{XY} is just the line segment XY . Let $P = Y - X$, and let P_X and P_\perp be its decomposition into the parts corresponding to Y_X and Y_\perp . Let Z be a point on XY denoted by $|e|_Z = |e|_X + \alpha p_e$. Let $Z_X = X + \alpha P_X$ and let $Z_\perp = X + \alpha P_\perp$ be the component of Z orthogonal to $\mathcal{O}(X)$. By

Cor. 6.2, the value of the directional derivative from X to Y_X is

$$(62) \quad F'(X, Y_X) = \lim_{\alpha \rightarrow 0} \frac{F(Z_X) - F(X)}{\alpha} = \sum_{e \in E_X} p_e [\nabla F(X)]_e$$

and the directional derivative from X to Y_\perp is

$$(63) \quad F'(X, Y_\perp) = \lim_{\alpha \rightarrow 0} \frac{F(Z_\perp) - F(X)}{\alpha}$$

$$(64) \quad = 2 \sum_{i=1}^n \left(\sum_{l: \|A_l^i\|_X=0} \left(\|B_l^i\| \sqrt{\sum_{e \in A_l^i} p_e^2} \right) - \sum_{e \in C^i \setminus E_X} |e|_{T^i} p_e \right) \quad \square$$

Proof of Thm. 4.4

Proof. The starting point for proving this claim will be analysis of the difference of function values $F'(X, Y^\alpha) - F'(X, Y)$. Lem. 6.7 states the value of the directional derivative can be expressed by any valid support sequences. Lem. 6.8 states the directional derivative is a continuous function of Y . Taken together these lemmas imply that the values of both $F'(X, Y^\alpha)$ and $F'(X, Y)$ can be expressed using any valid geodesic support sequences for the geodesic from T^i to Y^α , when α is small enough. The difference of function values, $F'(X, Y^\alpha) - F'(X, Y)$ simplifies to

$$(65) \quad F'(X, Y^\alpha) - F'(X, Y) = \sum_{e \in E_X} \alpha(|e|_{Y'} - |e|_Y) [\nabla F(X)]_e$$

$$(66) \quad - \sum_{e \in C^i \setminus E_X} \alpha(|e|_{Y'} - |e|_Y) |e|_{T^i}$$

$$(67) \quad + \sum_{i=1}^n \sum_{l: \|A_l^i\|_X=0} (\|A_l^i\|_{Y^\alpha} - \|A_l^i\|_Y) \|B_l^i\|_{T^i}.$$

Splitting terms on line (66) into two cases (i) when $e \in (C^i \setminus E_X) \cap E_Y$ (ii) when $e \in C^i \setminus E_Y$ and splitting terms on line (67) into two cases, (i) when $\|A_l^i\|_Y > 0$ and (ii) when $\|A_l^i\|_Y = 0$ yields

$$(68) \quad F'(X, Y^\alpha) - F'(X, Y) = \sum_{e \in E_X} \alpha(|e|_{Y'} - |e|_Y) [\nabla F(X)]_e$$

$$(69) \quad - \sum_{e \in (C^i \setminus E_X) \cap E_Y} \alpha(|e|_{Y'} - |e|_Y) |e|_{T^i}$$

$$(70) \quad - \sum_{e \in C^i \setminus E_Y} \alpha(|e|_{Y'} - |e|_Y) |e|_{T^i}$$

$$(71) \quad + \sum_{i=1}^n \sum_{\substack{l: \|A_l^i\|_X=0 \\ \|A_l^i\|_Y > 0}} (\|A_l^i\|_{Y^\alpha} - \|A_l^i\|_Y) \|B_l^i\|_{T^i}$$

$$(72) \quad + \sum_{i=1}^n \sum_{\substack{l: \|A_l^i\|_X=0 \\ \|A_l^i\|_Y=0}} (\|A_l^i\|_{Y^\alpha} - \|A_l^i\|_Y) \|B_l^i\|_{T^i}.$$

Now the difference, $F'(X, Y^\alpha) - F'(X, Y)$ is simplified to a state where it is convenient to

analyze the derivative, that is,

$$(73) \quad \lim_{\alpha \rightarrow 0} \frac{F'(X, Y^\alpha) - F'(X, Y)}{\alpha} = \sum_{e \in E_X} (|e|_{Y'} - |e|_Y) [\nabla F(X)]_e$$

$$(74) \quad - \sum_{e \in (C^i \setminus E_X) \cap E_Y} (|e|_{Y'} - |e|_Y) |e|_{T^i}$$

$$(75) \quad - \sum_{e \in C^i \setminus E_Y} (|e|_{Y'} - |e|_Y) |e|_{T^i}$$

$$(76) \quad + \sum_{i=1}^n \sum_{l : \|A_l^i\|_X = 0} \sum_{\substack{e \in A_l^i \\ \|A_l^i\|_Y > 0}} |e|_Y (|e|_{Y'} - |e|_Y) \frac{\|B_l^i\|_{T^i}}{\|A_l^i\|_Y}$$

$$(77) \quad + \sum_{i=1}^n \sum_{l : \substack{\|A_l^i\|_X = 0 \\ \|A_l^i\|_Y = 0}} \|A_l^i\|_{Y'} \|B_l^i\|_{T^i}.$$

Taking partial derivatives of $F'(X, Y)$ shows that the sum of terms on lines (73), (74), and (76) is equal to $\sum_{e \in E_Y} (|e|_{Y'} - |e|_Y) [\nabla F'(X, Y)]_e$. One can verify, by using the formula for the value of the directional derivative, Thm. 6.6, that the sum of terms on lines (75) and (77) is equal to $F'(Y, Y'_{\perp \mathcal{O}(Y)})$. \square

Proof of Thm. 4.5

Proof. If $F'(Y^{k-1}, Y^k) \geq 0$ and $\nabla F'(Y^{k-2}, Y^{k-1}) \perp \Delta^i$ then Y^{k-1} is a minimizer of $F'(Y^{k-2}, Y)$ in $\mathcal{O}(E)$. By induction, Y^1 is a minimizer of $F'(Y^0, Y)$ in $\mathcal{O}(E)$. Since $F'(Y^0, Y) \geq 0$, Y^0 is a minimizer of $F(X)$ in $\mathcal{O}(E)$.

Now the other direction is proved. If Y^0 is optimal in $\mathcal{O}(E)$, then there exists a minimizer, Y^1 of $F'(Y^0, Y)$ which satisfies the assumptions of the theorem. Inductively, the minimizer, Y^{i+1} , of $F'(Y^i, Y)$ must also satisfy the assumptions of the theorem. \square

7. Concluding remarks and research directions. We obtained relative optimality conditions and algorithms for optimizing the Fréchet function in an orthant of treespace. However, a further challenge remains - a method to quickly verify a point is optimal with respect to all orthants which contain it. The sheer number of orthants which contain a point may be very large with respect to the data, however this is not an indication that there are no polynomial certificates. In fact, an indicator this problem is not NP-complete is randomized split-proximal point algorithms produce sequences of points with expected distances to the Fréchet mean converging to zero at a linear rate, and no approximation methods with such a rate of convergence exists for NP-complete optimization problems e.g. weighted clique problems. One interesting direction is to research why the maximum clique problem is harder (or not harder) than finding the orthant of treespace, or equivalently a clique in the split-split compatibility graph (see Sec. 2.2), which contains the Fréchet mean.

Another area of interest is accelerating existing optimization techniques. One way to accelerate Fréchet optimization is to speed up geodesics optimization. Notice that the systems of equations defining pre-vistal facets and pre-vistal cells are quadratic cones with cone points at the origin of treespace. In squared treespace, the vistal facets and vistal cells are polyhedral cones. Multi-vistal facets are also polyhedral cones with cone points at the origin of treespace because they are intersections of polyhedral cones share a cone point at the origin of treespace. The nice geometric structure of vistal cells could be useful for determining when a search point is on the boundary of a vistal cell, and thus when the objective function has multiple forms. Therefore the geometry and combinatorics of vistal cells are a mathematical basis for methods to dynamically update the objective function during line searches. Such dynamic updating is a topic of further research, and will be the focus of a separate paper.

The necessity to define a fixed set of labeled leaves to use BHV Treespace limits applications. The space of treeshapes [8] relaxes the requirement for labeled leaves and generalizes the attributes of edges from scalars to vectors. However this flexibility comes at the cost of much more challenging optimization problems. Effective and robust methods for problems, such as computing geodesics and means, are not yet available.

In phylogenetics, when the root of the tree is a common ancestor, there is often a condition that the path in the tree from the root to each other leaf is maintained to a fixed constant. BHV treespace is also a superset of such trees. An interesting research direction is optimizing the Fréchet mean subject to constraints on the edges of the target tree.

Acknowledgments. We would like to acknowledge the assistance of SIOPT Editors and anonymous reviewers for peer review of this article and their advice.

REFERENCES

- [1] M. BAČÁK, *The proximal point algorithm in metric spaces*, Israel Journal of Mathematics, 194 (2013), pp. 689–701.
- [2] M. BAČÁK, *Computing medians and means in hadamard spaces*, SIAM Journal on Optimization, 24 (2014), pp. 1542–1566.
- [3] M. BAČÁK, *Convex analysis and optimization in Hadamard spaces*, vol. 22, Walter de Gruyter GmbH & Co KG, 2014.
- [4] M. BAČÁK, *A novel algorithm for computing the Fréchet mean in Hadamard spaces*, <http://arxiv.org/pdf/1210.2145v1.pdf> (2012), (2012).
- [5] D. P. BERTSEKAS, *Incremental proximal methods for large scale convex optimization*, Mathematical Programming, 129 (2011), pp. 163–195, <https://doi.org/10.1007/s10107-011-0472-0>, <http://link.springer.com/10.1007/s10107-011-0472-0>.
- [6] L. BILLERA, S. HOLMES, AND K. VOGTMANN, *Geometry of the space of phylogenetic trees*, Adv. in Appl. Math, 27 (2001), pp. 733–767.
- [7] J. FELSENSTEIN, *Inferring Phylogenies*, Sinauer Associates Inc., 2004.
- [8] A. FERAGEN, P. LO, M. DE BRUIJNE, M. NIELSON, AND F. LAUZE, *Towards a theory of statistical tree-shape analysis*, IEEE Transactions on Pattern Analysis and Machine Intelligence, 20 (2012).
- [9] A. FERAGEN, J. PETERSEN, M. OWEN, P. LO, L. H. THOMSEN, M. M. WILLE, A. DIRKSEN, AND M. DE BRUIJNE, *A hierarchical scheme for geodesic anatomical labeling of airway trees*, in Medical Image Computing and Computer-Assisted Intervention—MICCAI 2012, Springer, 2012, pp. 147–155.
- [10] O. GASCUEL, *Mathematics of evolution and phylogeny*, OUP Oxford, 2005.
- [11] M. B. GERSTEIN, C. BRUCE, J. S. ROZOWSKY, D. ZHENG, J. DU, J. O. KORBEL, O. EMANUELSSON, Z. D. ZHANG, S. WEISSMAN, AND M. SNYDER, *What is a gene, post-encode? history and updated definition*, Genome research, 17 (2007), pp. 669–681.
- [12] S. HOLMES, *Statistics for phylogenetic trees*, Theoretical population biology, 63 (2003), pp. 17–32.
- [13] S. HOLMES, *Statistical approach to tests involving phylogenies*, Mathematics of Evolution and Phylogeny, (2005), pp. 91–120.
- [14] B. R. LARGET, S. K. KOTHA, C. N. DEWEY, AND C. ANÉ, *Bucky: gene tree/species tree reconciliation with bayesian concordance analysis*, Bioinformatics, 26 (2010), pp. 2910–2911.
- [15] C. LI, G. LOPEZ, AND V. MARTIN-MARQUEZ, *Monotone vector fields and the proximal point algorithm on Hadamard manifolds*, Journal of the London Mathematical Society, 79 (2009), pp. 663–683, <https://doi.org/10.1112/jlms/jdn087>, <http://jlms.oxfordjournals.org/cgi/doi/10.1112/jlms/jdn087>.
- [16] W. P. MADDISON, *Gene trees in species trees*, Systematic biology, 46 (1997), pp. 523–536.
- [17] E. MILLER, M. OWEN, AND J. S. PROVAN, *Polyhedral computational geometry for averaging metric phylogenetic trees*, Advances in Applied Mathematics, 68 (2015), pp. 51–91, <https://doi.org/10.1016/j.aam.2015.04.002>, <http://dl.acm.org/citation.cfm?id=2791584.2791902>.
- [18] M. OWEN, *personal communication*, 2014.
- [19] M. OWEN AND S. PROVAN, *A fast algorithm for computing geodesic distances in tree space*, Computational Biology and Bioinformatics, 8 (2011), pp. 2–13.
- [20] R. T. ROCKAFELLAR, *Monotone Operators and the Proximal Point Algorithm*, SIAM Journal on Control and Optimization, 14 (1976), pp. 877–898, <https://doi.org/10.1137/0314056>, <http://epubs.siam.org/doi/abs/10.1137/0314056>.
- [21] S. SKWERER, E. BULLITT, S. HUCKEMANN, E. MILLER, I. OGUZ, M. OWEN, V. PATRANGENARU, S. PROVAN, AND J. S. MARRON, *Tree-Oriented Analysis of Brain Artery Structure*, Journal of Mathematical Imaging and Vision, (2014), <https://doi.org/10.1007/s10851-013-0473-0>, <http://link.springer.com/10.1007/s10851-013-0473-0>.
- [22] K. STURM, *Probability measures on metric spaces of nonpositive curvature, in heat kernels and analysis on manifolds, graphs, and metric spaces: lecture notes from a quarter program on heat kernels, random walks, and analysis on manifolds and graphs*, 338 (2003), pp. 357–390.